



# *Toxoplasma gondii* acetyl-CoA synthetase is involved in fatty acid elongation (of long fatty acid chains) during tachyzoite life stages<sup>S</sup>

David Dubois, Stella Fernandes, Souad Amiar, Sheena Dass, Nicholas J. Katris, Cyrille Y. Botté,<sup>1,2</sup> and Yoshiaki Yamaryo-Botté<sup>1,2</sup>

ApicoLipid Team, Institute of Advanced Biosciences, CNRS UMR5309, Université Grenoble Alpes, INSERM U1209, Grenoble, France

ORCID IDs: 0000-0002-2245-536X (C.Y.B.)

**Abstract** Apicomplexan parasites are pathogens responsible for major human diseases such as toxoplasmosis caused by *Toxoplasma gondii* and malaria caused by *Plasmodium* spp. Throughout their intracellular division cycle, the parasites require vast and specific amounts of lipids to divide and survive. This demand for lipids relies on a fine balance between de novo synthesized lipids and scavenged lipids from the host. Acetyl-CoA is a major and central precursor for many metabolic pathways, especially for lipid biosynthesis. *T. gondii* possesses a single cytosolic acetyl-CoA synthetase (TgACS). Its role in the parasite lipid synthesis is unclear. Here, we generated an inducible TgACS KO parasite line and confirmed the cytosolic localization of the protein. We conducted <sup>13</sup>C-stable isotope labeling combined with mass spectrometry-based lipidomic analyses to unravel its putative role in the parasite lipid synthesis pathway. We show that its disruption has a minor effect on the global FA composition due to the metabolic changes induced to compensate for its loss. However, we could demonstrate that TgACS is involved in providing acetyl-CoA for the essential fatty elongation pathway to generate FAs used for membrane biogenesis. **■** This work provides novel metabolic insight to decipher the complex lipid synthesis in *T. gondii*.—Dubois, D., S. Fernandes, S. Amiar, S. Dass, N. J. Katris, C. Y. Botté, and Y. Yamaryo-Botté. *Toxoplasma gondii* acetyl-CoA synthetase is involved in FA elongation (of long FA chains) during tachyzoite life stages. *J. Lipid Res.* 2018. 59: 994–1004.

**Supplementary key words** fatty acid synthesis and elongation • apicoplast • membrane biogenesis • lipidomics • stable isotope labeling

Apicomplexa are unicellular eukaryotes, of which most member organisms are obligate intracellular parasites. The Apicomplexa phylum comprises important human pathogens

such as *Toxoplasma gondii*, causing toxoplasmosis, and *Plasmodium* spp., the causative agent of malaria. These pathogens represent a global human and social threat against which there is no efficient vaccine and which are becoming increasingly resistant to all marketed drugs, especially in the case of *Plasmodium falciparum*, the major agent of lethal human malaria (1). There is a pressing need for the identification of new drug targets and for the development of novel inhibitors.

Understanding the complex metabolic pathways by which these parasites can obtain the nutrients essential for their survival is an important avenue for drug development. Specifically, lipid synthesis is a pivotal and essential pathway for the parasite during its intracellular development for membrane biogenesis, proper lipid homeostasis, and lipid signaling. Due to its complex and unique evolution, the lipid synthesis pathway is highly compartmentalized and forms a puzzle pathway with enzymes of different origins. Indeed, most Apicomplexa (with the exception of *Cryptosporidium*) harbor a relict nonphotosynthetic plastid named the apicoplast (Apicomplexa plastid) (2, 3), which has been acquired by the secondary endosymbiosis of a red algal ancestor (4). Similarly, as in plant and algal plastids, the apicoplast contains a prokaryotic type II FA synthesis pathway (FASII pathway) that is essential in both

This work was supported by Agence Nationale de la Recherche Grant ANR-12-PDOC-0028 – Project Apicolipid; the Centre National de la Recherche Scientifique Atip-Avenir and Finovi programs; and the Laboratoire d'Excellence Parafra Grant ANR-11-LABX-0024. C.Y.B. is a Centre National de la Recherche Scientifique Atip-Avenir Fellow.

Manuscript received 21 December 2017 and in revised form 30 March 2018.

Published, JLR Papers in Press, April 20, 2018

DOI <https://doi.org/10.1194/jlr.M082891>

Abbreviations: ACCase, acetyl-CoA carboxylase; ACL, ATP-citrate lyase; ACS, acetyl-CoA synthetase; ATc, anhydrotetracycline; BCKDH, branched-chain keto acid dehydrogenase; ER, endoplasmic reticulum; FAME, FA methyl ester; FASII, type II FA synthesis; HA, hemagglutinin; HFF, human foreskin fibroblast; IFA, immunofluorescence assay; LPA, lysophosphatidic acid; MID, mass isotopomer distribution; PDH, pyruvate dehydrogenase; PyK, pyruvate kinase; SeACS, *Salmonella enterica* ACS; TgACL, *Toxoplasma gondii* ACL; TgACS, *Toxoplasma gondii* ACS; TgACS-iKO, inducible knockdown of TgACS.

<sup>1</sup>C. Y. Botté and Y. Yamaryo-Botté contributed equally to this work.

<sup>2</sup>To whom correspondence should be addressed.

e-mail: cyrille.botte@univ-grenoble-alpes.fr or

cyrille.botte@gmail.com (C.Y.B.); yoshiaki.yamaryo@gmail.com (Y.Y.B.)

**S** The online version of this article (available at <http://www.jlr.org>) contains a supplement.

Copyright © 2018 by the American Society for Biochemistry and Molecular Biology, Inc.

This article is available online at <http://www.jlr.org>

*T. gondii* and *P. falciparum* (5–10). The apicoplast also has the capacity to use FASII FAs and form lysophosphatidic acid (LPA) and phosphatidic acid, which are crucial precursors used for bulk membrane biogenesis and for the survival of the parasite (5, 8, 10–15). Apicoplast-generated FAs and LPAs are then exported toward the endoplasmic reticulum (ER), where they can be elongated and desaturated by elongases and dehydratase to expand the FA range used to maintain the parasite lipid homeostasis in each of its intracellular compartments (7, 14, 16).

In addition to these de novo lipid synthesis pathways, parasites are also capable of scavenging lipids and other resources from the host and the external environment. The parasite lipid synthesis, composition, and homeostasis depend on a fine-tuning between the de novo synthetic pathways, the scavenged lipid moieties, and the trafficking of these lipids. Furthermore, parasites can sense the availability of lipids and other nutrients from the environment to modulate the balance between de novo and scavenging metabolic pathways and thus maintain membrane biogenesis, proper growth, division, and thus survival and pathogenesis (17–19).

Acetyl-CoA is a crucial metabolite in the central carbon metabolism of Apicomplexan parasites, including lipid synthesis and the mitochondrial TCA cycle (7, 17, 20–23). Indeed, the main precursor of the apicoplast FASII is acetyl-CoA, which is generated via the apicoplast pyruvate dehydrogenase (PDH) (6). The apicoplast PDH is fueled via the import of phosphoenolpyruvate, which is generated via the cytosolic glycolysis pathway and then transported via the apicoplast phosphate transporter [also named the apicoplast triose phosphate transporter in *P. falciparum* (7, 17)], in a similar manner as in plant plastids (24–27). The ER FA elongation pathway also requires acetyl-CoA as a carbon source to elongate the apicoplast-generated FAs. Unlike plants and most eukaryotes, Apicomplexan mitochondria lack a canonical PDH to synthesize acetyl-CoA, essential for the TCA cycle (20). Instead, the parasite uses a branched-chain keto acid dehydrogenase (BCKDH) that possesses a dual function to also make acetyl-CoA for the TCA cycle (20, 28). In *T. gondii*, acetyl-CoA can also be made via a cytosolic ATP-citrate lyase (*TgACL*) using a by-product of the TCA cycle, oxaloacetate, unlike *P. falciparum*, which seems to lack a homolog of *TgACL*. However, both *T. gondii* and *P. falciparum* possess a single acetyl-CoA synthetase (ACS) that can use acetate imported from the host and/or the external environment for acetyl-CoA by active transfer of acetate to the CoA (21). Recent analysis of the *T. gondii* ACS and ATP-citrate lyase (ACL) showed that each enzyme is dispensable alone but that the dual-KO parasite strain for *TgACS* and *TgACL* is not viable (28). Taken together, these data point at the importance of acetyl-CoA and its synthesis in the metabolism of these parasites. To date, no metabolomic analysis has been performed to unravel the metabolic role of *TgACL*, and especially *TgACS*, which is the sole enzyme capable of using a scavenged substrate, i.e., acetate, for acetyl-CoA synthesis.

Here, we generated an inducible knockdown of the *T. gondii* ACS, *TgACS*-iKO. We conducted state-of-the-art

stable isotope labeling, using  $^{13}\text{C}$ -U-glucose and  $^{13}\text{C}$ -U-acetate, combined with mass spectrometry-based lipidomic analysis of the *TgACS*-iKO to determine its putative role in FA synthesis and FA elongation, respectively. We report that the enzyme contributes to the parasite lipid synthesis pathways, specifically for the elongation of FA by the ER elongases, whereas it does not participate in the de novo synthesis pathways for FA synthesis. This is the first report that *TgACS* has a role beyond being a source of acetyl-CoA for protein acylation and histone acylation and shows the versatility of the parasite to confront its metabolic demand and nutrient availabilities.

## MATERIALS AND METHODS

### Sequence analysis and structure generation

*TgACS* gene (TGGT1-266640) was identified by using toxoDB (<http://toxodb.org/toxo/>), and alignment with *S. enterica* was performed on Multalin (<http://multalin.toulouse.inra.fr/multalin/multalin.html>) (29). The 3D structure was determined via protein threading against the previously crystallized *S. enterica* ACS (30), using SwissProt bioinformatics (<https://swissmodel.expasy.org/>).

### *T. gondii* strains and cultures

*T. gondii* tachyzoites [RH- $\Delta$ Ku80 TATi (31) and *TgACS*-iKO-HA] were maintained in human foreskin fibroblasts (HFFs) using DMEM (Gibco) supplemented with 1% FBS (Gibco), 2 mM glutamine (Gibco), and 25  $\mu\text{g}/\text{ml}$  gentamicin (Gibco) at 37°C and 5%  $\text{CO}_2$ .

### Construct design

*TgACS* (TGGT1-266640) gene sequences were obtained from ToxoDB. The *TgACS* open reading frame was PCR-amplified using primers 5'-GAAGATCT ATGGAGAAAGATAGGAACACTATG-GAGGG and 5'-TGGCCTAGGAGCTTTCGCA-AGAGAGCCCC. *TgACS* untranslated flanking regions were generated using the following primers: 5'UTR: 5'-GGAATTCATATGTACTTCCACAT-ACGTCTGCTTGTGC and 5'-GGAATTCATATGGGTGTTCC-TGGTCTGAAATGTTGC and the 3' UTR: with 5'-AT-ACCCGG-GACGATTTATACACATGGTTAGACCAGGC and 5'-ATAAGAAT-GCG-GCCGCACGTCCTTCATTAGCCATCTGTTGC. PCR was performed using PrimeSTAR Max DNA Polymerase (TaKaRa, Japan) denaturing at 98°C for 10 s and annealing at 60°C for 10 s and extension at 72°C (1 min/kbp). These PCR products were then inserted into the vector pDt7s4H (Fig. 1B) (32, 33). The resulting construct was transfected into *T. gondii* RH Ku80\_TATi strain parasites as described (14). Transfected parasites were then selected on pyrimethamine and cloned. Mutant clones with successful replacement of the native *TgACS* gene locus with the resistant cassette and inducible promoter together with CDS was confirmed by PCR using their genomic DNA as template and following primers as indicated in Fig. 2: Primer1, 5'-AACGCA-CACACAAATGCTCC\_3'; Primer2, 5'-GCGTCGTTTTTGTCC-ACGA\_3'; Primer3, 5'-ACGAACCATGTCGA-GGCTTT\_3'; Primer4, 5'-CGTAG-TCCGGGACATCGTAC\_3'; Primer5, 5'-GTACGATG-TCCCGGACTACG\_3'; and Primer6, 5'-ACCTTCATAGAGGCA-GCCGA\_3'.

### Antibodies and IFAs

Primary anti-CPN60 (rabbit) antibodies were used at a dilution of 1/6,000 and anti-HA at 1/1,000 (mouse, Invivogen). Secondary Alexa Fluor 488- and 546-conjugated anti-mouse and anti-rabbit antibodies (Life Technologies) were used at 1/10,000. Parasites

were grown on confluent HFF on coverslips and fixed in PBS containing 4% paraformaldehyde for 30 min at room temperature (RT). Samples were permeabilized with 0.1% Triton X-100 in PBS for 10 min at RT before blocking in PBS containing 3% BSA and incubation with primary antibodies, then secondary antibodies diluted in the blocking solution. Labeled parasites were stained with Hoechst (1/10,000, Life Technologies) for 20 min and then washed three times in PBS, then H<sub>2</sub>O. Coverslips were mounted onto slides prior to observation using an epifluorescent microscope (Zeiss, Germany).

### Western blotting

Protein expression was analyzed by Western blot on freshly egressed parasites. Equal amounts (50 µg) of protein were boiled in SDS-PAGE buffer separated on a 4–12% gradient SDS-polyacrylamide (Life Technologies) and transferred to PVDF membrane (Millipore) using the XCellIII Blot Module (Invitrogen). The membrane was blocked with skim milk and then probed with monoclonal mouse anti-HA antibodies (InvivoGen) at 1:2,000 and mouse anti-Gra1 antibodies at 1:3,000. Secondary goat anti-mouse HRP conjugated antibodies (Thermo Scientific) were used at 1:20,000. Signal was detected after membrane staining with the Luminata Crescendo Western HRP detection kit (Millipore).

### Phenotypic analysis

Plaque assays were performed with 500 parasites infected to HFF confluent monolayers in culture flasks (25 cm<sup>2</sup>). *TgACS*-HA-iKO parasites were grown in the presence or absence of ATc 0.5 µg/ml for 10 days. Then, cells were fixed with ethanol, followed by staining with Crystal Violet (Sigma).

### Lipid extraction from *T. gondii* tachyzoites and GC/MS analysis

Intracellular tachyzoites (1 × 10<sup>8</sup> cell equivalents per replicate) were harvested after metabolic quenching in dry ice-ethanol (100%) to rapidly stop the metabolism as previously described (7, 34). Then total lipids were extracted in chloroform/methanol/water [1:3:1, vol/vol/vol containing 25 nmol tridecanoic acid (C13:0) as internal standard for extraction] for 1 h at 4°C, with periodic sonication. Then polar and apolar metabolites were separated by phase partitioning. For lipid analysis, the organic phase was dried under N<sub>2</sub> gas and dissolved in chloroform/methanol, 2:1 (vol/vol). Then, the lipid was mixed with 1 nmol of pentadecanoic acid (C15:0) as internal standard and derivatized using MethPrep II (Alltech). The resulting FAMES were analyzed by GC/MS as previously described (7, 34). All FAMES were identified by comparison of retention time and mass spectra from GC/MS with authentic chemical standards. Then FAMES were normalized to cell number and extraction efficiency and quantified. The experiments were repeated as indicated using each independent mutant line as a biological replicate.

### Stable isotope metabolic labeling of *T. gondii* FAs

Stable isotope metabolic labeling experiment using U-<sup>13</sup>C-glucose or U-<sup>13</sup>C-acetate (Cambridge Isotope Laboratories), followed by lipid extraction and GC/MS analysis was performed as previously described (7, 14, 34). Parasites were infected to confluent HFF and incubated in the presence or absence of ATc (2 µM, Sigma-Aldrich). For the change of <sup>13</sup>C labeling in the course of *TgACS*-HA suppression by ATc, glucose-free medium supplemented with a U-<sup>13</sup>C-glucose or U-<sup>13</sup>C-acetate at a final concentration of 8 mM was used concomitant with the inoculation of parasites, and parasites were harvested after 4 days. For the

change of <sup>13</sup>C labeling after the loss of *TgACS* protein by ATc, parasites were grown for 72 h in the normal medium. Then, medium was replaced with glucose-free medium supplemented with <sup>13</sup>C-U-carbon source (concentration as above), while presence or absence of ATc was maintained. At 24 h of the incubation with <sup>13</sup>C source medium, parasites were harvested for the lipid analysis as described above. Other supplements (glutamine, sodium bicarbonate, and FBS) were added according to normal culture conditions; minimal concentration of <sup>12</sup>C-glucose (800 µM final concentration) was added to the cultures for <sup>13</sup>C-U-acetate labeling experiment. All lipids were then analyzed by GC/MS after derivatization using Methprep II (Alltech). Mass shift in each mass spectra of each FA were analyzed to assess the incorporation of <sup>13</sup>C to FAs.

## RESULTS

### *TgACS* is a cytosolic protein that is not essential during the tachyzoite stage

In order to identify the role of ACS, we first searched for a candidate ACS in *T. gondii* genome using the ToxoDB website (<http://toxodb.org/toxo/>). We found a predicted gene annotated as ACS (accession no. TGGT1-266640) based on sequence homology with other characterized ACSs (35–37). The candidate protein was bearing typical domains for ACS, such as AMP binding (PF13193) and CoA binding (TIGR02188). Comparison of *TgACS* protein sequence against the ACS of *Salmonella enterica*, *SeACS*, the protein of which was crystallized (30), showed a high level of conservation between the two proteins. Indeed, alignment showed a 52% identity over 91% of the protein covered when comparing *SeACS* to *TgACS*. Most residues involved in CoA binding (i.e., F222, A223, G224, R250, K253, I255, A417, S585, G586, H587, R588, K642, and R646) and AMP binding (i.e., I370, V446, T472, Y473, W474, 8475, T476, E477, and I574) (**Fig. 1A**) are identical or highly conserved as well. Furthermore, we searched for homologs of ACS in *P. falciparum* and the chromerids, *Chromera velia* and *Vitrella brassicaformis*, and found putative candidates, *PfACS* (PF3D7\_0627800, the enzyme likely responsible for the acetyl-CoA synthesis from acetate described in ref. 21), *CvACS* (Cve1\_1982), and *VbACS* (VBra\_8944), respectively. We compared those to protein sequence of *SeACS*, *TgACS*, and human ACS, which showed that there is a high homology among these divergent organisms (supplemental Fig. S1). This, added to the fact that recombinant *HsACS* was shown to generate acetyl-CoA from acetate (38), strongly supports that the *TgACS* gene locus is encoding for an active ACS. We furthermore performed in silico protein threading (or homology modeling) against the crystal structure of *S. enterica*. Predicted *TgACS* structure can merge together with that of *S. enterica* and conserves the structural amino acid localization of predicted substrates binding CoA and AMP with high scores and confidence from the prediction software. This high structural conservation is indicative of an important and fundamental requirement of ACS in the cellular function and homology to characterized ACS (**Fig. 1B–F**).



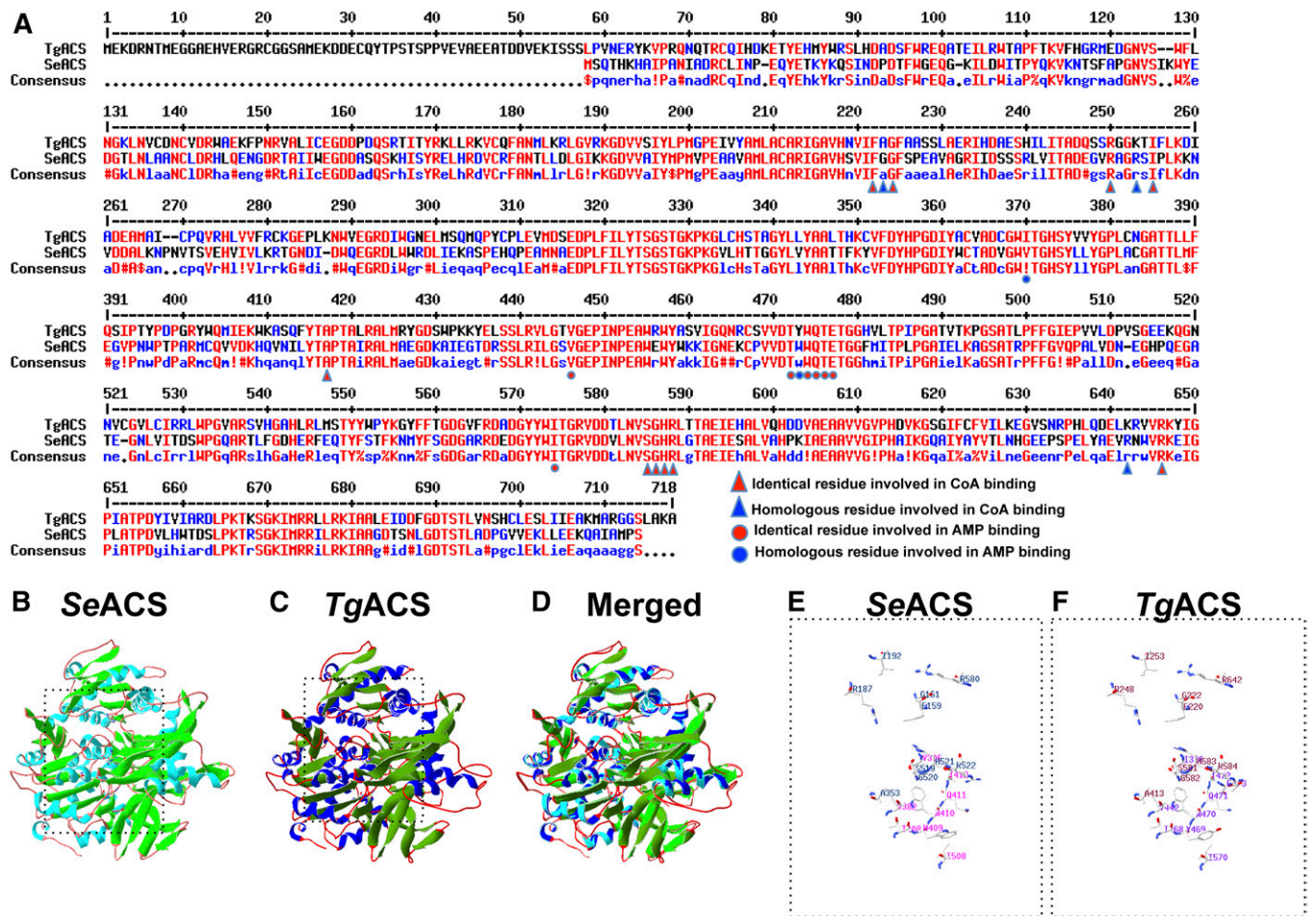


**Fig. 1.** Structural analysis of the predicted *TgACS*. **A:** Alignment of protein sequences from *TgACS* and *SeACS*. High consensus or identity in the residues are shown in red and lower consensus is shown in blue, while black depicts neutrality. Amino acid residues for the CoA binding are depicted by red triangles, homologous residues for the CoA binding are shown with blue triangles, identical residues involved in AMP binding are shown by red circles, and homologous residues for AMP binding are shown with blue circles. **B:** Crystal structure of *SeACS*. **C:** Predicted model of *TgACS* based on *SeACS* crystal structure. **D:** Overlay of the *SeACS* crystal structure and the homology model of *TgACS*. The overall structure of *TgACS* is conserved and highly similar as observed in the ribbon representation. **E:** A 3D representation of the amino acid residues involved in AMP and CoA in *SeACS*. **F:** A 3D representation of the predicted residues involved in AMP and CoA binding in *TgACS*.

In order to localize *TgACS*, we generated a construct that expressed *TgACS* fused to a C-terminal triple hemagglutinin (3×HA) epitope tag under control of an anhydrotetracycline (ATc)-regulated promoter (*TgACS*-HA-iKO; **Fig. 2A–C**). This *TgACS*-HA-iKO strain enabled us to analyze the effect of disruption of *TgACS*. Two independent mutants were generated within a *T. gondii* TATi\_Δ*Ku80* background (31), and the successful replacement of the endogenous locus was confirmed via PCR (**Fig. 2C**). Immunofluorescence assays (IFAs) using anti-HA antibody showed that *TgACS*-HA was localized within the cytosol of the parasite similarly to previous reports (28, 39) (**Fig. 3A**, upper). The effect of repression of *TgACS* was observed by IFA after the addition of ATc (0.5 μg/ml) to the parasite culture (**Fig. 3A**, lower). The addition of ATc led to significant loss of HA signal within 2 days after the treatment with ATc (**Fig. 3A**), suggesting that *TgACS* most likely is not essential for in vitro growth for parasites.

We then analyzed the effect of ATc on the *TgACS*-HA protein level via Western blot analysis. *TgACS*-HA protein was detected as a single distinct band with an apparent

molecular mass of 80 kDa, corresponding to its predicted molecular mass of 79.8 kDa. The addition of 0.5 μg/ml ATc to the culture medium downregulated *TgACS*-HA expression, and the protein was undetectable after 3 days of ATc treatment (**Fig. 3B**). This kinetics complements the rapid loss of *TgACS*-HA signal observed during IFA.

While the loss of *TgACS*-HA did not affect parasite morphology, we investigated possible growth defects through plaque assays. The knockdown of *TgACS* led to no discernable alteration in plaque size, so ATc treatment of the parental lines produced no detectable growth retardation (**Fig. 3C, D**). This suggested that *TgACS* is not essential, in accordance with a recent genomewide analysis of essential genes in *Toxoplasma* by CRISPR-Cas9 KO, which pointed to the likely nonessential role of *TgACS* (40).

#### *TgACS* disruption slightly alters the total FA content of the parasite

Since the ACS gene encodes for an enzyme to produce acetyl-CoA, a major precursor for FA synthesis and FA elongation, it is possible that loss of *TgACS* may alter the lipid

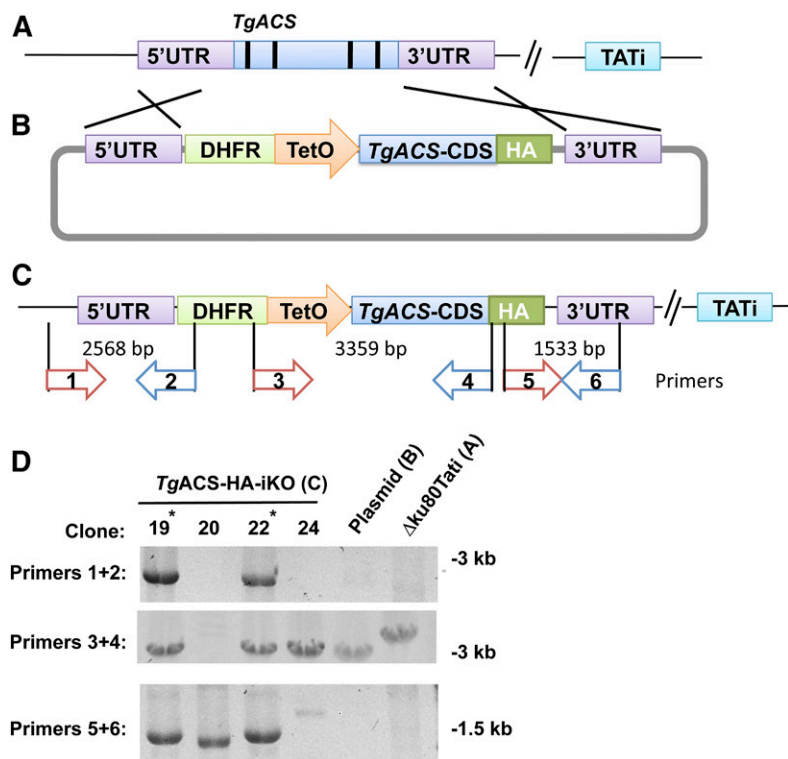


**Fig. 2.** Generating *TgACS*-HA-iKO. A: A tetracycline-regulated transactivator (TATi) expressing strain. B: Modified pDT7s4H plasmid for promoter replacement and tagging. C: Modified gene locus and primers used for D. D: Confirmation of replacement of gene locus by PCR.

profile of the parasite. We first qualified and quantified the FA content in the *TgACS*-HA-iKO parasite in the absence and presence of ATc for 4 days. FA moieties of glycerolipids were derivatized to FA methyl ester (FAME), and then FAMES were quantified by GC/MS (catalog no. 5977A-7890B, Agilent Technology). There was no major difference in total FA content between the reference and induced *TgACS* KO strains (Fig. 4A). However, slight differences in the FA composition could be detected (Fig. 4B, C). Although *TgACS* can generate acetyl-CoA that is hypothesized to be used for the elongation of FAs, there was slight yet nonsignificant decrease in the longer-chain FA amount known to be produced via the elongation pathway (7), such as C20:1, C22:1, and C24:1. Interestingly, however, in the ATc-treated parasite, the apicoplast FASII-generated C12:0 and C14:0 were decreased significantly, while C22:6, a FA source believed to be scavenged from the host, was significantly increased.

#### ***TgACS* disruption does not impair apicoplast FA synthesis**

To determine the potential role of *TgACS* for FA synthesis, including de novo FA synthesis in the apicoplast and FA elongation in the ER, we performed metabolic labeling on ATc-treated and untreated *TgACS*-iKO-HA parasites with stable isotope precursors, i.e.,  $^{13}\text{C}$ -universally labeled carbon substrate,  $\text{U-}^{13}\text{C}$ -glucose, or  $\text{U-}^{13}\text{C}$ -acetate, respectively. These substrates can be incorporated to the parasites and are used for the FA synthesis in different pathways (7, 14, 41). Incorporation of  $^{13}\text{C}$ -glucose to FAs determines the de novo synthesized FAs via FASII in apicoplast (7, 14, 41), whereas the incorporation of  $^{13}\text{C}$ -acetate FAs determines the elongation of FAs in cytosol (7, 16). The resulting labeled FAs can be distinguished by the shift of mass by GC/MS. The degree of the incorporation of  $^{13}\text{C}$  into FAs (% carbon incorporation) is determined by the mass isotopomer distribution (MID) of

each FAME. These together can delineate the exact effect on lipid metabolism of *TgACS* knockdown. MID can be obtained from the shift in isotopic mass dependent on the amount of  $^{12}\text{C}$  carbons compared with the integration of  $^{13}\text{C}$  carbon atoms. For example, myristic acid (C14:0) consists of a carbon backbone of 14 carbons in length; the most common isotope would contain only  $^{12}\text{C}$  with a detectable mass-to-charge ratio of  $m/z$  228; as no  $^{13}\text{C}$  has been incorporated, we call this isotope mass 0 (M0). Integration patterns vary from one carbon to fully labeled; incorporation of four  $^{13}\text{C}$  leads to an increase in mass by four,  $M+4$ ,  $m/z$  232. These isotopic distributions allow us to determine the metabolic flux and processes involved in lipid biosynthesis.

To investigate the role *TgACS* in the de novo lipid synthesis, we first labeled *TgACS*-HA-iKO parasites with  $\text{U-}^{13}\text{C}$ -glucose for 4 days continuously with ATc to disrupt *TgACS*, similar to the condition analyzed for the total FA composition (Fig. 4). Labeling for 4 days of ATc treatment and labeling with  $\text{U-}^{13}\text{C}$ -glucose showed no significant alteration for  $^{13}\text{C}$  incorporation for all the FA species analyzed (Fig. 5A). MID analysis of C14:0 showed the typical two by two mass increase up to the  $M+14$  mass due to  $^{13}\text{C}$  from 6 carbon glucose was metabolized to 2 carbon acetyl-CoA in the apicoplast (Fig. 5B). This two by two went up to  $M+14$  to show the full synthesis of C14:0 by the apicoplast FASII as we previously reported (14). Similarly, the MID analysis of C20:0 showed the full synthesis up to  $M+14$  and  $M+16$ , mainly correlating the origin of C20:0 from the apicoplast FASII major products C14:0 and C16:0 (Fig. 5C) (7, 14).

Since 4 days of labeling still includes 2 days of expression of active *TgACS* protein (Fig. 3B), most of the  $^{13}\text{C}$ -carbon integration may have occurred before the loss of *TgACS*, potentially masking obvious difference between the knockdown mutant and its parental line. To measure the direct



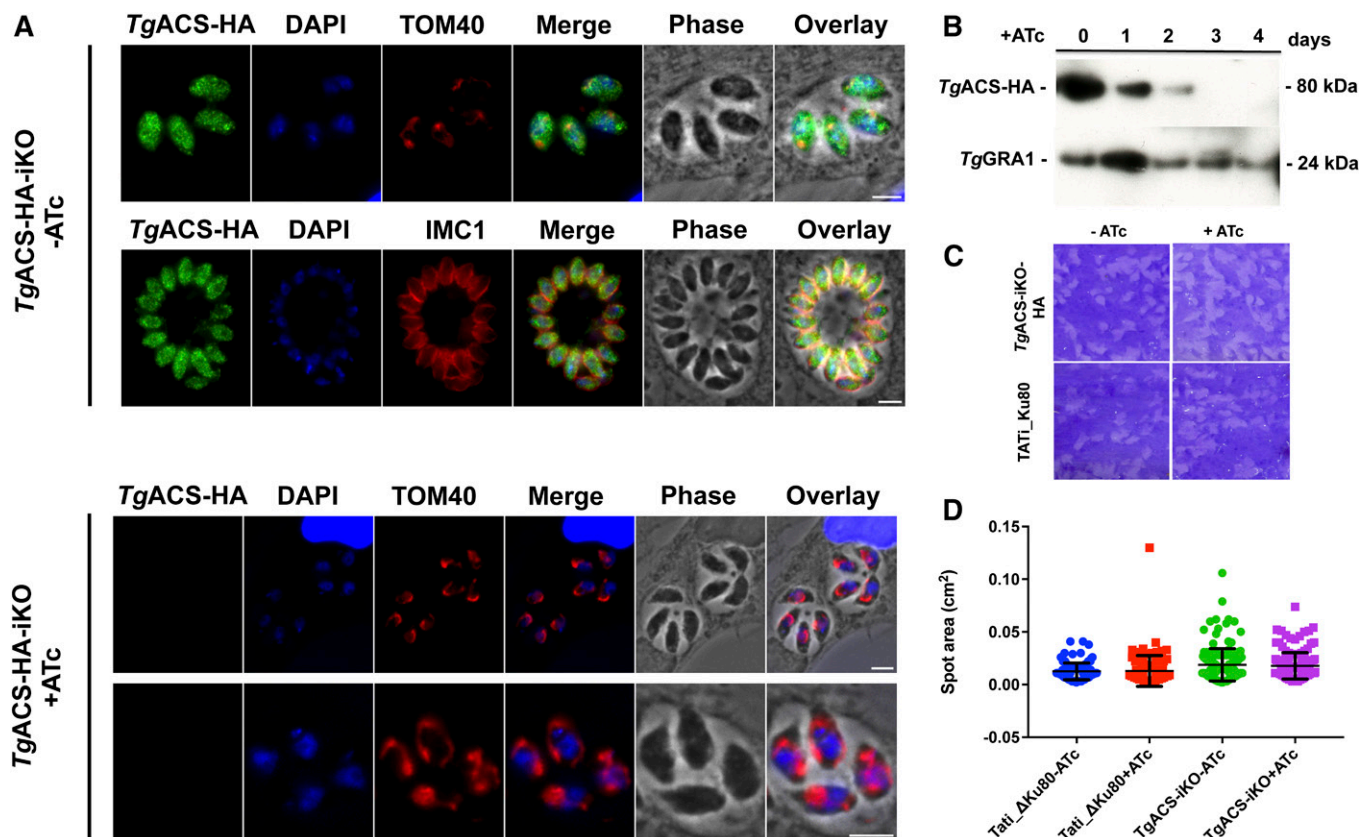


**Fig. 3.** *TgACS-HA-iKO* is a dispensable cytosolic protein that can be downregulated to determine its cellular function. **A:** IFA images of *TgACS-HA-iKO* strain with or without ATc. *TgACS-HA* fluorescent signal is shown in green. DAPI, as a marker for the nucleus, is shown in blue. IMC1 and TOM40 are markers of the inner membrane complex and the parasite mitochondria, respectively, and both are shown in red. *TgACS-HA* localizes in the cytosol, and this signal is lost after the addition of ATc. **B:** Western blotting image of *TgACS-HA-iKO* strain. *TgACS-HA* protein is detected at the predicted molecular mass, 79.8 kDa. The addition of ATc causes complete protein loss after 3 days. **C:** Plaque assays were used to evaluate the growth of the *TgACS-HA-iKO* strains with or without ATc in comparison to *T. gondii* reference strain, Tati-Ku80. **D:** Statistical analysis of plaque assay was performed to show that there was no difference in the presence or absence of *TgACS* protein. All scale bars, 5  $\mu$ m.

effect of loss of *TgACS*, we grew parasites with or without ATc for 48 h prior to the addition of U- $^{13}$ C-glucose (pretreatment 2 days). Then, parasites were incubated with U- $^{13}$ C-glucose for the next 72 h. In this condition, overall incorporation of  $^{13}$ C-carbon integration was reduced to approximately half of 4 day labeling (Fig. 5D). Here, again, there was no significant difference between ATc-treated and nontreated parasites in the integration of  $^{13}$ C-carbon in FAs from glucose. In addition, the integration pattern of  $^{13}$ C to apicoplast generated FAs, C14:0, showed clear two by two increase of mass up to M+14 in both conditions (Fig. 5E), suggesting that there was no activation or alteration of FASII upon the loss of *TgACS*. MID analysis of C14:0, however, showed a significant reduction of  $^{13}$ C incorporation in the M+12 and M+14 isotopologues in the *TgACS* knockdown mutant. This slight reduction of relative abundance for the M+14 (and M+12) could be a sign of slight reduction of the FASII activity.

#### *TgACS* disruption significantly alters the ER FA elongation pathway

To investigate whether acetyl-CoA generated by *TgACS* is involved in the elongation of FA, we first labeled parasites with U- $^{13}$ C-acetate continuously for 4 days with or without ATc (Fig. 6). In this condition, there was incorporation of

$^{13}$ C label to all FAs analyzed both with and without ATc. Interestingly, the  $^{13}$ C incorporation from acetate to shorter FAs, C14:0 and C16:0, in the *TgACS-HA-iKO* with ATc was significantly higher than that without ATc (Fig. 6A). In the meantime,  $^{13}$ C incorporation to longer FAs known to be products of the elongation pathway, especially C18:1, C20:0, and C20:1, was significantly reduced (Fig. 6A). MID analysis of  $^{13}$ C integration into C14:0 and C16:0 showed that the measured labeling increase displayed an unusual pattern of M+1 incorporation from M+2 to M+8 (Fig. 6B, C). However, there was no sign of two by two increase of the mass, which was seen in the U- $^{13}$ C-glucose as signature of apicoplast FASII, suggesting that acetate was not directly incorporated into the apicoplast as a substrate for FASII, but rather that acetate was catabolized to a single carbon molecule and then metabolized to be used in the FASII pathway. MID analysis of C20:0 did not show clear increase of M+2, M+4, a usual signature for the elongation pathway (Fig. 6D). Although  $^{13}$ C incorporation from acetate was altered, there was no total abrogation of such incorporation. Taken together, this also suggests that 4 days of incubation with U- $^{13}$ C-acetate with or without ATc was likely too long and may not be the best-suited approach to determine effect of the loss of *TgACS*.

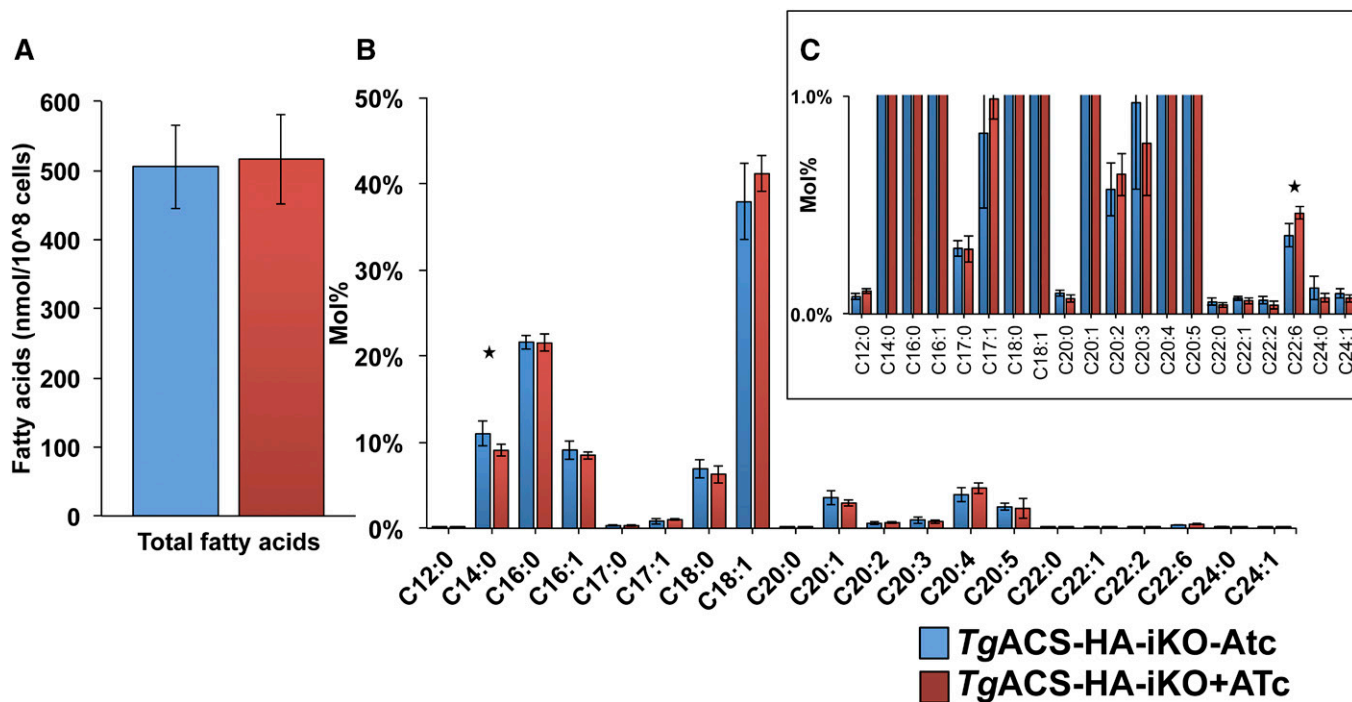


**Fig. 4.** Total FA composition in *TgACS-HA-iKO*. A: Total lipids were extracted from *TgACS-HA-iKO* grown with or without ATc for 4 days. Then, total lipid was derivatized with MethprepII to give FAME, and their amount was quantified by GC/MS following normalization according to internal standards (C14:0) and cell numbers. B: Relative abundance of FAs. C: Magnified view of B. *TgACS-HA-iKO-ATc* (blue) and *TgACS-HA-iKO+ATc* (n = 6). \*  $P < 0.05$ .

We thus treated parasites with ATc for 2 days prior to addition of U-<sup>13</sup>C-acetate and grown for a further 2 days (pretreatment 2 days) to suppress most of the *TgACS* present in the parasite. In this condition, <sup>13</sup>C integration from <sup>13</sup>C-acetate was almost abrogated in most long FA chains C18:0, C20:0, C22:0, and C24:0 generated via the elongation pathway (Fig. 6E). Here, no incorporation of <sup>13</sup>C to C14:0 or

C16:0 in both strains was observed (Fig. 6F, G), suggesting that what observed in Fig. 6B and C was probably due to the catabolism of acetate due to long incubation in the course of *TgACS* deactivation. The MID analysis of C20:0 showed a clear increase of M+2, and M+4, in the absence of ATc (i.e., WT condition), which is the signature of elongation of the FASII products C18:0 and C16:0 (14). However, in the

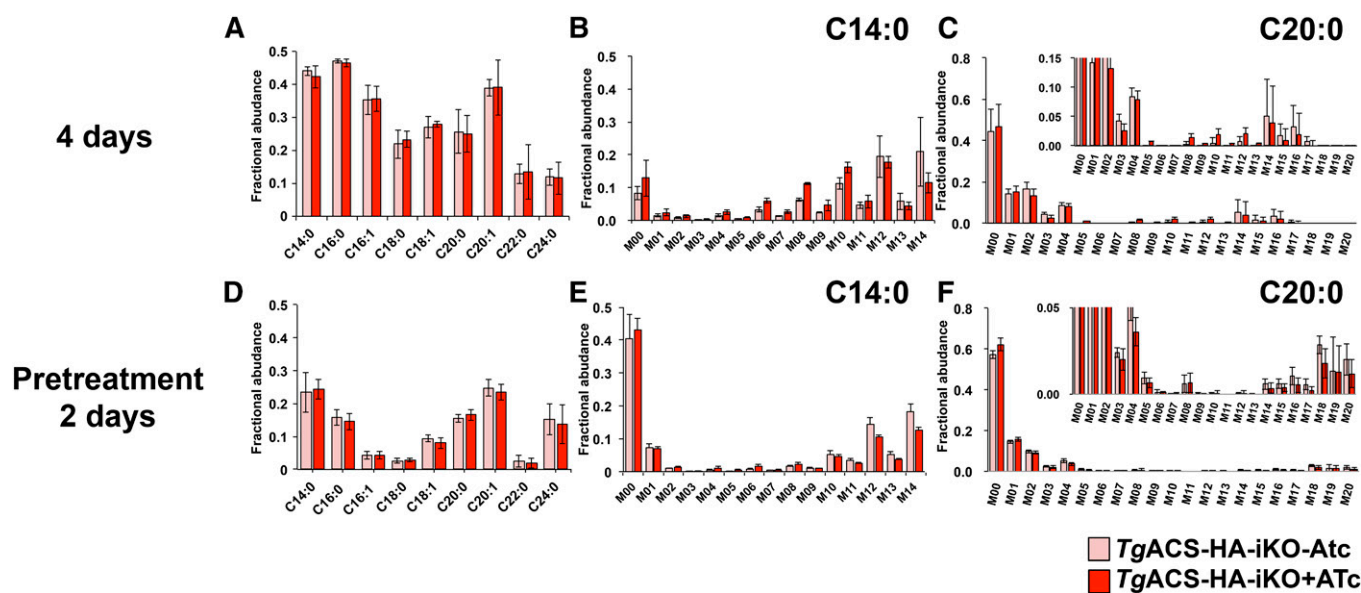


**Fig. 5.** Determination of the *TgACS* putative role in de novo FA synthesis via the apicoplast FASII. A–C: *TgACS-HA-iKO* was grown in the presence of U-<sup>13</sup>C-glucose simultaneously with or without ATc for 4 days. A: %<sup>13</sup>C carbon integration to each FA species. B: MID of C14:0. C: MID for C20:0 (n = 4). D–F: *TgACS-HA-iKO* was grown with or without ATc for 2 days prior to the addition of U-<sup>13</sup>C-glucose and grown for a further 2 days. D: %<sup>13</sup>C carbon integration to each FA species. E: MID for C14:0. F: MID for C20:0. *TgACS-HA-iKO-ATc*, pale red, and *TgACS-HA-iKO+ATc*, dark red (n = 7).

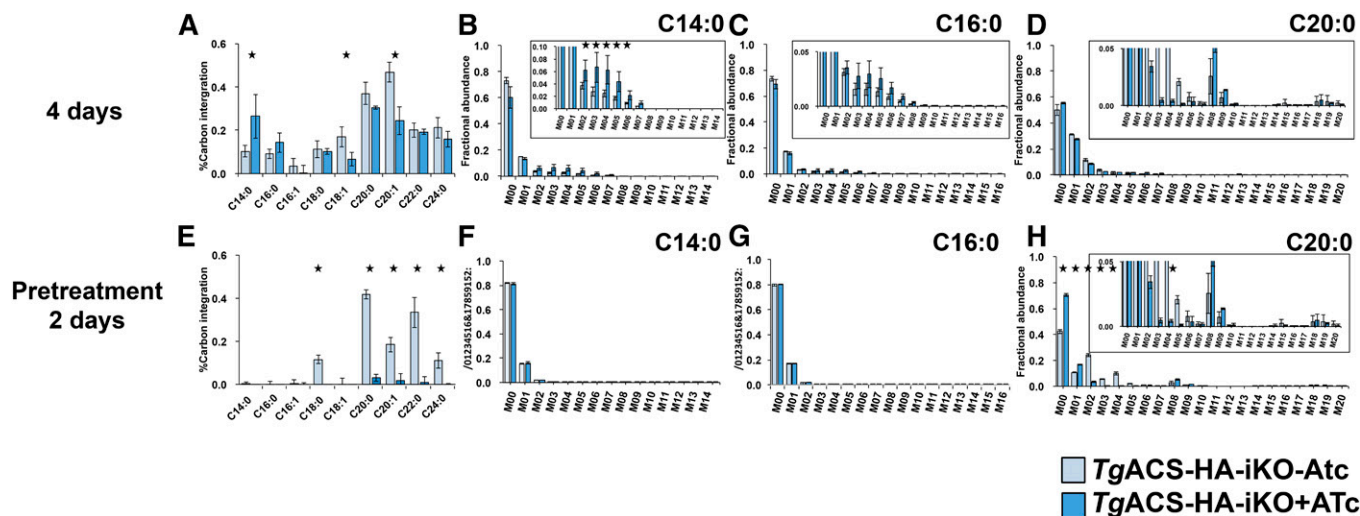


**Fig. 6.** Determination of *TgACS* putative role for FA elongation. A–D: *TgACS*-HAiKO was grown in the presence of U-<sup>13</sup>C-acetate simultaneously with or without ATc for 4 days. A: %<sup>13</sup>C carbon integration to each FA species B: MID of C14:0. C: MID for C16:0. D: MID for C20:0. (n = 3) E–H: *TgACS*-HAiKO was grown with or without ATc prior to the addition of U-<sup>13</sup>C-acetate to grow a further 2 days E: %<sup>13</sup>C carbon integration to each FA species. F: MID for C14:0 G: MID for C16:0. H: MID for C20:0. *TgACS*-HAiKO-ATc, pale red, and *TgACS*-HAiKO+ATc, dark red. (n = 5). \* *P* < 0.05.

presence of ATc, i.e., lack of *TgACS*, labeled C20:0 did not contain any increase of M+2 and M+4 (Fig. 6H). This clearly suggests that the loss of *TgACS* could not provide the substrate, acetyl-CoA, for the elongation of FAs. Similar results were measured for the other altered FA chains, suggesting that C18:0 is elongated from C16:0, C22:0 from C18:0 and C16:0, C20:1 predominantly from C18:1 mainly and slightly from C16:1/0 and C24:0, C16:0, and C14:0 (supplemental Fig. S2). Collectively, these metabolic results indicate that the loss of *TgACS* leads to a reduction in the elongation of FA by the lack of acetyl-CoA it produces for the pathway.

## DISCUSSION

In this study, we determined the role of the sole enzyme capable of generating acetyl-CoA from a scavenged substrate (i.e., acetate) for lipid synthesis in *T. gondii*. Indeed, acetyl-CoA is a central metabolite that is involved in the TCA cycle, FA synthesis, FA elongation, and posttranslational protein acylation, including histone acylation for genetic regulation. The apicoplast FASII pathway generates its own pool of acetyl-CoA via the apicoplast PDH, and the mitochondrial BCKDH generates the acetyl-CoA required to initiate the TCA cycle (28). The source and role of acetyl-CoA for cytosolic FA synthesis via the FASI pathway and the ER elongation pathway remain to be fully understood. Previous studies showed that *T. gondii* possesses two enzymes capable of generating acetyl-CoA: the ACS (*TgACS*) and the ACL (28). Where *TgACS* is theoretically capable of using acetate and binds it to CoA, *TgACL* uses existing citrate from the TCA to generate acetyl-CoA. Interestingly the localization of *TgACS* shows a uniform cytosolic and nuclear localization, as previously described (28, 39). The nuclear localization supports the potential role of *TgACS* for providing acetyl-CoA in the nucleus for histone acetylation. Further analysis to determine its putative role in histone modification and chromatin remodeling by

determining *T. gondii* acetylome on the *TgACS*-iKO mutant would be important to conduct. Here, we disrupted *TgACS* and were able to determine its role in generating acetyl-CoA for FA biosynthesis.

The loss of *TgACS* disrupts the typical mechanism of FA elongation, which relies on three elongases together essential for parasite survival (7). Here, our results clearly demonstrate that the acetyl-CoA generated by *TgACS* is used by the elongases to contribute to the production of many elongated FAs initially produced by the apicoplast FASII (C18:0, C18:1, C20:0, C20:1, C22:0, and C24:0) (Fig. 7; ref. 14). The lack of major changes in the FA composition and the nonlethal phenotype of *TgACS*-iKO mutant clearly support the presence of another source of acetyl-CoA for the essential FA elongation pathway. This is likely a redundant role of *TgACL*, as previously shown when both *TgACS* and *TgACL* were knocked out, which eventually killed the parasite (28). This hypothesis is also strengthened by the increase of ACL abundance when *TgACS* is disrupted (28). Interestingly, *P. falciparum* seems to lack a homolog to the citrate lyase and possesses the sole ACS to generate acetyl-CoA from acetate (21), which seems essential for the parasite (42). Further analyses are a prerequisite to understand the differences between *T. gondii* and *P. falciparum* lipid synthesis and use of acetyl-CoA.

Genetic ablation of *TgACS* does not kill the parasite; however, metabolic plasticity enables continued parasite survival via providing alternate substrate options maintaining elongation at a suitable level, as measured by the absence of major changes in the total FA composition. As an evidence of such compensation, upon the loss of *TgACS*, C12:0 and C14:0, major products of FASII (14), decrease, while C22:6, a FA chain believed to be scavenged (7, 43), increases. When we incubated parasites with <sup>13</sup>C-U-acetate for 4 days, the incorporation of labeling was observed in both *TgACS*-iKO with or without ATc, although <sup>13</sup>C-U-acetate was not supposed to be used as substrate for the de novo FA



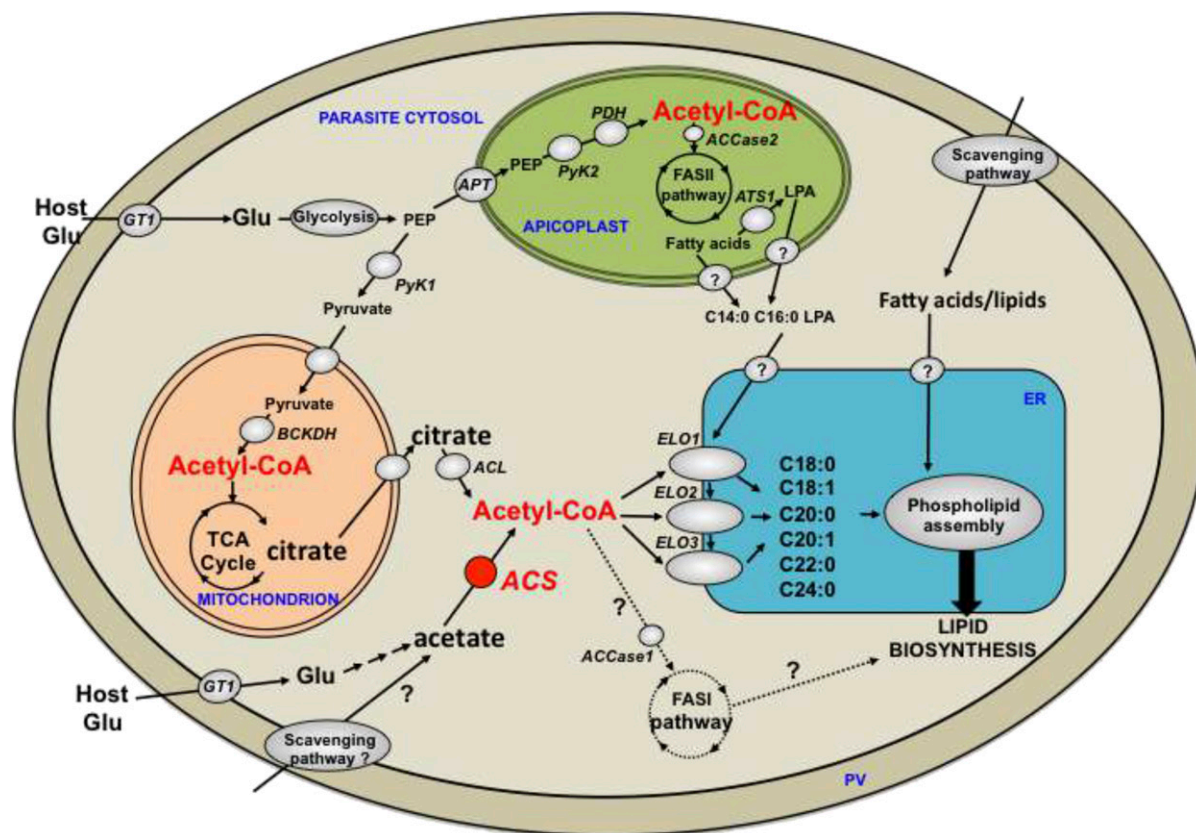


**Fig. 7.** Proposed role of *TgACS* and acetyl-CoA in the lipid biosynthetic pathway of *T. gondii* tachyzoite. Acetyl-CoA can be generated by the cytosolic ACS using acetate as a substrate. This pool of acetyl-CoA is used as a substrate for the parasite elongases (ELO1, 2, 3) in the ER to form C18:0, C18:1, C20:0, C20:1, C22:0, and C24:0. These elongated FAs are used to generate phospholipids for the bulk lipid biosynthetic pathways along with the FASII-derived FA and lipid precursor (LPA) made in the apicoplast and the FAs and lipids scavenged from the host. The origin of acetate used by ACS partially derives from metabolized glucose, while another fraction is likely scavenged from the host environment. Acetyl-CoA can also be generated via cytosolic ACL, which uses citrate made by the mitochondrial TCA cycle, and that is exported into the cytosol. This pool of acetyl-CoA can most likely be used by the elongation pathway as a possible redundant route to ACS function in elongation. FAs generated by the apicoplast FASII are the major substrates for the ER elongases. Acetyl-CoA is also made from glycolytic intermediates phosphoenolpyruvate (PEP) and pyruvate by the apicoplast PDH and the mitochondrial BCKDH for the FASII pathway and the mitochondrial TCA cycle, respectively. Theoretically, acetyl-CoA generated by ACS and ACL could fuel the cytosolic FASI pathway but our current results suggest that this is not the case during tachyzoite life stages. APT, apicoplast phosphate transporter; ATS1, apicoplast glycerol-3-phosphate acyltransferase; ELO, elongase; Glu, glucose; GT1, glucose transporter; PV, parasitophorous vacuole.


synthesis, i.e., incorporation to short-chain FAs, C14:0 FAs. In addition, the labeling in C14:0 was more abundant upon the loss of *TgACS*, suggesting that the parasite enhanced some metabolic pathway and used acetate for de novo A synthesis upon the loss of *TgACS*. First of all, it should be noted that both *TgACS*-iKO with or without ATc had incorporation of  $^{13}\text{C}$ -U-acetate to C14:0 only up to M+7 and to C16:0 only up to M+8 in each mass. Therefore, parasites only had half of their carbon chains being labeled with  $^{13}\text{C}$ . Furthermore, incorporation of  $^{13}\text{C}$  was done in a “continuous manner” without the typical two-by-two carbon incorporation occurring through FA elongation. This was only observed when parasites were incubated for 4 days with  $^{13}\text{C}$ -U-acetate with or without ATc, but not in 2 days, even in the -ATc condition. This suggests that acetate was not directly used for the TCA cycle similarly as shown in *Plasmodium*, that  $^{13}\text{C}$ -labeled acetate is rapidly incorporated to acetyl-CoA and then to acetylated alanine and acetylated glutamate but not to keto-glutarate, a TCA intermediate (21). It

is possible that acetate was recycled from those acetylated amino acid to be metabolized to pyruvate, probably via TCA cycle to serve as a precursor for the de novo FA synthesis. Another potential explanation for these is that the unused acetate was catabolized to give a single carbon molecule, bicarbonate, and  $\text{CO}_2$  to be used in another metabolic pathway. Finally, *T. gondii* is able to generate propionyl-CoA from the degradation of leucine, isoleucine, and valine (44). This propionyl-CoA is toxic for the cell and needs to be detoxified. One alternative way to degrade it would be through its utilization as a substrate in place of acetyl-CoA, which would potentially explain the +1 increase that we measured (Fig. 6).

Interestingly, accumulation of acetate in rats has been shown to downregulate the expression of lipogenic genes such as *a*) pyruvate kinase (PyK), which catalyzes the synthesis of pyruvate for the generation of acetyl-CoA for FA synthesis by the FAS; *b*) acetyl-CoA carboxylase (ACCase), which catalyzes the synthesis of malonyl-CoA the other essential

substrate for the FAS pathways (both type I and II); and *c*) FAS (45). All of these enzymes are present in *T. gondii* and could putatively be regulated by an accumulation of acetate following *TgACS* disruption; PyK is present in two essential isoforms in *T. gondii*, *TgPyKI*, likely in the cytosol, and *TgPyKII*, dually localized in the mitochondrion and the apicoplast (46, 47), ACCase is also present in two copies: one in the apicoplast to fuel the FASII and one likely in the cytosol potentially for FASI and/or elongases (48). Furthermore, it has also been shown that ACCase can be downregulated when there is the accumulation of the FASII products (49). So it is possible that the accumulation of C14:0 that is not elongated anymore due to the lack of acetyl-CoA provided by *TgACS* could indeed inhibit the FASII pathway as we observed in this work. Similarly, the abrogation of  $^{13}\text{C}$  incorporation from acetate in C18:1 in the 2 days pretreatment (Fig. 6E) might be explained by a massive scavenging of C18:1 from the external environment to compensate for the loss of its synthesis via the elongation pathway. Altogether, our observations conclude that *TgACS* loss perturbed the FA metabolism, causing modification of lipid balance in the induced KO due to its role in providing acetyl-CoA for FA elongation.

One of the important questions that remains unanswered is the origin of the acetate used by *TgACS*. In human blood, it is said to contain 50–200  $\mu\text{M}$  acetate. Here, in vitro, supplemented FBS also contains certain amount acetate (50), but this is possibly irrelevant because, thus far, no transporter for acetate has been identified in Apicomplexa. Furthermore,  $^{13}\text{C}$ -glucose labeling in *P. falciparum* shows that a small part of the intracellular acetate pool originates from glucose but that most of it is of unknown origin (21). Although acetate can be found in the extracellular environment, its origin in Apicomplexa might not be from importing it, but may be as a downstream product of host or parasite metabolism.

In summary, we demonstrated that *a*) *TgACS* is a nonessential enzyme present as a uniform protein of the cytosol and likely the nucleus; *b*) it does not participate in providing substrate for the de novo synthesis of FA by the apicoplast FASII; *c*) its disruption does not have much influence over the parasite FA composition; but *d*) it provides acetyl-CoA for the elongation of FA and actively participates in this pathway, which is essential for parasite survival (7). These data show for the first time that one of the enzymes capable of the synthesis of acetyl-CoA is also involved in the parasite lipid synthesis and the plasticity of *T. gondii* to compensate for the loss of proteins participating in these crucial pathways for membrane biogenesis. 

## REFERENCES

- World Health Organization 2017. World malaria report 2017. World Health Organization, Geneva.
- McFadden, G. I., M. E. Reith, J. Munholland, and N. Lang-Unnasch. 1996. Plastid in human parasites. *Nature*. **381**: 482.
- Köhler, S., C. F. Delwiche, P. W. Denny, L. G. Tilney, P. Webster, R. J. Wilson, J. D. Palmer, and D. S. Roos, 1997. A plastid of probable green algal origin in apicomplexan parasites. *Science*. **275**: 1485–1489.
- Janouskovec, J., A. Horák, M. Oborník, J. Lukeš, and P. J. Keeling. 2010. A common red algal origin of the apicomplexan, dinoflagellate, and heterokont plastids. *Proc. Natl. Acad. Sci. USA*. **107**: 10949–10954.
- Waller, R. F., P. J. Keeling, R. G. Donald, B. Striepen, E. Handman, N. Lang-Unnasch, A. F. Cowman, G. S. Besra, D. S. Roos, and G. I. McFadden. 1998. Nuclear-encoded proteins target to the plastid in *Toxoplasma gondii* and *Plasmodium falciparum*. *Proc. Natl. Acad. Sci. USA*. **95**: 12352–12357.
- Mazumdar, J., E. H. Wilson, K. Masek, C. A. Hunter, and B. Striepen. 2006. Apicoplast fatty acid synthesis is essential for organelle biogenesis and parasite survival in *Toxoplasma gondii*. *Proc. Natl. Acad. Sci. USA*. **103**: 13192–13197.
- Ramakrishnan, S., M. D. Docampo, J. I. Macrae, F. M. Pujol, C. F. Brooks, G. G. van Dooren, J. K. Hiltunen, A. J. Kastaniotis, M. J. McConville, and B. Striepen. 2012. Apicoplast and endoplasmic reticulum cooperate in fatty acid biosynthesis in apicomplexan parasite *Toxoplasma gondii*. *J. Biol. Chem.* **287**: 4957–4971.
- Yu, M., T. R. S. Kumar, L. J. Nkrumah, A. Coppi, S. Retzlaff, C. D. Li, B. J. Kelly, P. A. Moura, V. Lakshmanan, J. S. Freundlich, et al. 2008. The fatty acid biosynthesis enzyme *FabI* plays a key role in the development of liver-stage malarial parasites. *Cell Host Microbe*. **4**: 567–578.
- van Schaijk, B. C. L., T. R. S. Kumar, M. W. Vos, A. Richman, G. J. van Gemert, T. Li, A. G. Eappen, K. C. Williamson, B. J. Morahan, M. Fishbaugher, et al. 2014. Type II fatty acid biosynthesis is essential for *Plasmodium falciparum* sporozoite development in the midgut of *Anopheles* mosquitoes. *Eukaryot. Cell*. **13**: 550–559.
- Vaughan, A. M., M. T. O'Neill, A. S. Tarun, N. Camargo, T. M. Phuong, A. S. Aly, A. F. Cowman, and S. H. Kappe. 2009. Type II fatty acid synthesis is essential only for malaria parasite late liver stage development. *Cell. Microbiol.* **11**: 506–520.
- Fichera, M. E., and D. S. Roos. 1997. A plastid organelle as a drug target in apicomplexan parasites. *Nature*. **390**: 407–409.
- He, C. Y., M. K. Shaw, C. H. Pletcher, B. Striepen, L. G. Tilney, and D. S. Roos. 2001. A plastid segregation defect in the protozoan parasite *Toxoplasma gondii*. *EMBO J.* **20**: 330–339.
- Lindner, S. E., M. J. Sartain, K. Hayes, A. Harupa, R. L. Moritz, S. H. Kappe, and A. M. Vaughan. 2014. Enzymes involved in plastid-targeted phosphatidic acid synthesis are essential for *Plasmodium yoelii* liver-stage development. *Mol. Microbiol.* **91**: 679–693.
- Amiar, S., J. I. Macrae, D. L. Callahan, D. Dubois, G. G. van Dooren, M. J. Shears, M-F. Cesbron-Delauw, E. Maréchal, M. J. McConville, G. I. McFadden, et al. 2016. Apicoplast-localized lysophosphatidic acid precursor assembly is required for bulk phospholipid synthesis in *Toxoplasma gondii* and relies on an algal/plant-like glycerol 3-phosphate acyltransferase. *PLoS Pathog.* **12**: e1005765.
- Shears, M. J., J. I. Macrae, V. Mollard, C. D. Goodman, A. Sturm, L. M. Orchard, M. Llinás, M. J. McConville, C. Y. Botté, and G. I. McFadden. 2017. Characterization of the *Plasmodium falciparum* and *P. berghei* glycerol 3-phosphate acyltransferase involved in FASII fatty acid utilization in the malaria parasite apicoplast. *Cell. Microbiol.* **19**: e12633.
- Ramakrishnan, S., M. D. Docampo, J. I. Macrae, J. E. Ralton, T. Rupasinghe, M. J. McConville, and B. Striepen. 2015. The intracellular parasite *Toxoplasma gondii* depends on the synthesis of long-chain and very long-chain unsaturated fatty acids not supplied by the host cell. *Mol. Microbiol.* **97**: 64–76.
- Botté, C. Y., Y. Yamaryo-Botté, T. W. T. Rupasinghe, K. A. Mullin, J. I. Macrae, T. P. Spurck, M. Kalanon, M. J. Shears, R. L. Coppel, P. K. Crellin, et al. 2013. Atypical lipid composition in the purified relict plastid (apicoplast) of malaria parasites. *Proc. Natl. Acad. Sci. USA*. **110**: 7506–7511.
- Brancucci, N. M. B., J. P. Gerdt, C. Wang, M. De Niz, N. Philip, S. R. Adapa, M. Zhang, E. Hitz, I. Niederwieser, S. D. Boltryk, et al. 2017. Lysophosphatidylcholine regulates sexual stage differentiation in the human malaria parasite *Plasmodium falciparum*. *Cell*. **171**: 1532–1544.e15.
- Mancio-Silva, L., K. Slavic, M. T. Grilo Ruivo, A. R. Grosso, K. K. Modrzyńska, I. M. Vera, J. Sales-Dias, A. R. Gomes, C. R. MacPherson, P. Crozet, et al. 2017. Nutrient sensing modulates malaria parasite virulence. *Nature*. **547**: 213–216.
- Oppenheim, R. D., D. J. Creek, J. I. Macrae, K. K. Modrzyńska, P. Pino, J. Limenitakis, V. Polonais, F. Seeber, M. P. Barrett, O. Billker, et al. 2014. BCKDH: the missing link in apicomplexan mitochondrial metabolism is required for full virulence of *Toxoplasma gondii* and *Plasmodium berghei*. *PLoS Pathog.* **10**: e1004263.
- Cobbold, S. A., A. M. Vaughan, I. A. Lewis, H. J. Painter, N. Camargo, D. H. Perlman, M. Fishbaugher, J. Healer, A. F. Cowman, S. H. I. Kappe, et al. 2013. Kinetic flux profiling elucidates two independent acetyl-CoA biosynthetic pathways in *Plasmodium falciparum*. *J. Biol. Chem.* **288**: 36338–36350.

22. Foth, B. J., L. M. Stimmler, E. Handman, B. S. Crabb, A. N. Hodder, and G. I. McFadden. 2005. The malaria parasite *Plasmodium falciparum* has only one pyruvate dehydrogenase complex, which is located in the apicoplast. *Mol. Microbiol.* **55**: 39–53.
23. Pei, Y., A. S. Tarun, A. M. Vaughan, R. W. Herman, J. M. Soliman, A. Erickson-Wayman, and S. H. Kappe. 2010. *Plasmodium* pyruvate dehydrogenase activity is only essential for the parasite's progression from liver infection to blood infection. *Mol. Microbiol.* **75**: 957–971.
24. Mullin, K. A., L. Lim, S. A. Ralph, T. P. Spurck, E. Handman, and G. I. McFadden. 2006. Membrane transporters in the relict plastid of malaria parasites. *Proc. Natl. Acad. Sci. USA.* **103**: 9572–9577.
25. Karnataki, A., A. Derocher, I. Coppens, C. Nash, J. E. Feagin, and M. Parsons. 2007. Cell cycle-regulated vesicular trafficking of *Toxoplasma* APT1, a protein localized to multiple apicoplast membranes. *Mol. Microbiol.* **63**: 1653–1668.
26. Lim, L., M. Linka, K. A. Mullin, A. P. Weber, and G. I. McFadden. 2010. The carbon and energy sources of the non-photosynthetic plastid in the malaria parasite. *FEBS Lett.* **584**: 549–554.
27. Brooks, C. F., H. Johnsen, G. G. van Dooren, M. Muthalagi, S. S. Lin, W. Bohne, K. Fischer, and B. Striepen. 2010. The *Toxoplasma* apicoplast phosphate translocator links cytosolic and apicoplast metabolism and is essential for parasite survival. *Cell Host Microbe.* **7**: 62–73.
28. Tymoshenko, S., R. D. Oppenheim, R. Agren, J. Nielsen, D. Soldati-Favre, and V. Hatzimanikatis. 2015. Metabolic needs and capabilities of *Toxoplasma gondii* through combined computational and experimental analysis. *PLOS Comput. Biol.* **11**: e1004261.
29. Corpet, F. 1988. Multiple sequence alignment with hierarchical clustering. *Nucleic Acids Res.* **16**: 10881–10890.
30. Gulick, A. M., V. J. Starai, A. R. Horswill, K. M. Homick, and J. C. Escalante-Semerena. 2003. The 1.75 Å crystal structure of acetyl-CoA synthetase bound to adenosine-5'-propylphosphate and coenzyme A. *Biochemistry.* **42**: 2866–2873.
31. Sheiner, L., J. L. Demerly, N. Poulsen, W. L. Beatty, O. Lucas, M. S. Behnke, M. W. White, and B. Striepen. 2011. A systematic screen to discover and analyze apicoplast proteins identifies a conserved and essential protein import factor. *PLoS Pathog.* **7**: e1002392.
32. Agrawal, S., G. G. van Dooren, W. L. Beatty, and B. Striepen. 2009. Genetic evidence that an endosymbiont-derived endoplasmic reticulum-associated protein degradation (ERAD) system functions in import of apicoplast proteins. *J. Biol. Chem.* **284**: 33683–33691.
33. Agrawal, G. K., S. Tamogami, O. Han, H. Iwahashi, and R. Rakwal. 2004. Rice octadecanoid pathway. *Biochem. Biophys. Res. Commun.* **317**: 1–15.
34. MacRae, J. I., L. Sheiner, A. Nahid, C. Tonkin, B. Striepen, and M. J. McConville. 2012. Mitochondrial metabolism of glucose and glutamine is required for intracellular growth of *Toxoplasma gondii*. *Cell Host Microbe.* **12**: 682–692.
35. Starai, V. J., J. Garrity, and J. C. Escalante-Semerena. 2005. Acetate excretion during growth of *Salmonella enterica* on ethanolamine requires phosphotransacetylase (EutD) activity, and acetate recapture requires acetyl-CoA synthetase (Acs) and phosphotransacetylase (Pta) activities. *Microbiology.* **151**: 3793–3801.
36. Reger, A. S., J. M. Carney, and A. M. Gulick. 2007. Biochemical and crystallographic analysis of substrate binding and conformational changes in acetyl-CoA synthetase. *Biochemistry.* **46**: 6536–6546.
37. Hur, H., Y. B. Kim, I. H. Ham, and D. Lee. 2015. Loss of ACS2 expression predicts poor prognosis in patients with gastric cancer. *J. Surg. Oncol.* **112**: 585–591.
38. Luong, A., V. C. Hannah, M. S. Brown, and J. L. Goldstein. 2000. Molecular characterization of human acetyl-CoA synthetase, an enzyme regulated by sterol regulatory element-binding proteins. *J. Biol. Chem.* **275**: 26458–26466.
39. Nitzsche, R., V. Zagoriy, R. Lucius, and N. Gupta. 2016. Metabolic cooperation of glucose and glutamine is essential for the lytic cycle of obligate intracellular parasite *Toxoplasma gondii*. *J. Biol. Chem.* **291**: 126–141.
40. Sidik, S. M., D. Huet, S. M. Ganesan, M. H. Huynh, T. Wang, A. S. Nasamu, P. Thiru, J. P. J. Saeij, V. B. Carruthers, J. C. Niles, et al. 2016. A Genome-wide CRISPR Screen in *Toxoplasma* Identifies Essential Apicomplexan Genes. *Cell.* **166**: 1423–1435.e12.
41. Lévêque, M. F., L. Berry, Y. Yamaro-Botté, H. M. Nguyen, M. Galera, C. Y. Botté, and S. Besteiro. 2017. TgPL2, a patatin-like phospholipase domain-containing protein, is involved in the maintenance of apicoplast lipids homeostasis in *Toxoplasma*. *Mol. Microbiol.* **105**: 158–174.
42. Gomes, A. R., E. Bushell, F. Schwach, G. Girling, B. Anar, M. A. Quail, C. Herd, C. Pfander, K. Modrzynska, J. C. Rayner, et al. 2015. A genome-scale vector resource enables high-throughput reverse genetic screening in a malaria parasite. *Cell Host Microbe.* **17**: 404–413.
43. Welti, R., E. Mui, A. Sparks, S. Wernimont, G. Isaac, M. Kirisits, M. Roth, C. W. Roberts, C. Botté, E. Maréchal, et al. 2007. Lipidomic analysis of *Toxoplasma gondii* reveals unusual polar lipids. *Biochemistry.* **46**: 13882–13890.
44. Limenitakis, J., R. D. Oppenheim, D. J. Creek, B. J. Foth, M. P. Barrett, and D. Soldati-Favre. 2013. The 2-methylcitrate cycle is implicated in the detoxification of propionate in *Toxoplasma gondii*. *Mol. Microbiol.* **87**: 894–908.
45. Yamashita, H., K. Fujisawa, E. Ito, S. Idei, N. Kawaguchi, M. Kimoto, M. Hiemori, and H. Tsuji. 2007. Improvement of obesity and glucose tolerance by acetate in type 2 diabetic Otsuka Long-Evans Tokushima fatty (OLETF) rats. *Biosci. Biotechnol. Biochem.* **71**: 1236–1243.
46. Saito, T., M. Nishi, M. I. Lim, B. Wu, T. Maeda, H. Hashimoto, T. Takeuchi, D. S. Roos, and T. Asai. 2008. A novel GDP-dependent pyruvate kinase isozyme from *Toxoplasma gondii* localizes to both the apicoplast and the mitochondrion. *J. Biol. Chem.* **283**: 14041–14052.
47. Bakszt, R., A. Wernimont, A. Allali-Hassani, M. W. Mok, T. Hills, R. Hui, and J. C. Pizarro. 2010. The crystal structure of *Toxoplasma gondii* pyruvate kinase 1. *PLoS One.* **5**: e12736.
48. Jelenska, J., M. J. Crawford, O. S. Harb, E. Zuther, R. Haselkorn, D. S. Roos, and P. Gornicki. 2001. Subcellular localization of acetyl-CoA carboxylase in the apicomplexan parasite *Toxoplasma gondii*. *Proc. Natl. Acad. Sci. USA.* **98**: 2723–2728.
49. Faergeman, N. J., and J. Knudsen. 1997. Role of long-chain fatty acyl-CoA esters in the regulation of metabolism and in cell signaling. *Biochem. J.* **323**: 1–12.
50. Hosios, A. M., and M. G. Vander Heiden. 2014. Acetate metabolism in cancer cells. *Cancer Metab.* **2**: 27.